

//: Beyond the Plane

Larry C. Markley

Physics Department, The College of Wooster, Wooster, Ohio 44691, USA

(Dated: May 12, 2011)

This experiment continues work done on the // -body problem which investigates the interactions of two line segments (or slashes) confined to a plane. In this experiment the slashes are “freed” from the plane and, in doing so, add two more parameters in the form of polar angles, θ_A and θ_B . The addition of these parameters increases the complexity of the problem. However, the expressions for the potential energy and the equations of motion are found to be integrable. Visualization is also found to be possible though it was not within the scope of this experiment to do such visualizations beyond the potential energy.

I. INTRODUCTION

Over 300 years ago, Isaac Newton formulated his theory of gravitation. From this theory he was able to solve the two-body problem. The two body problem consists of essentially two point masses orbiting each other. Newton found that the stable orbits of these bodies were ellipses. Newton then approached what would seem to be the next logical step in orbital mechanics, the three-body problem. However, this proved to be much more complex than the two-body problem, in fact, it is *infinitely* more complex (Danby, 1988).

Since then, scientists such as Poincaré and many others have worked on the three-body problem and have found it to be chaotic. The three-body problem is a rich source of information on chaotic systems and this manifested in some of the pioneering work on chaos. One may ask, however, where is the distinction made? What is the critical point at which the two-body problem transcends simplicity? It was in the probing of these questions that work on this project began.

Previous work has been done on what is called the “2.5-body” problem, or /. (slash-dot) (Lindner, 2010). It is the exploration of the interaction between a point mass and a line segment that results in chaotic behavior. This experiment pushes that boundary even further by exploring the interaction of two line segments. In previous work, Alex Saines derived the potential energy and equations of motion for the two line segments (or slashes) as they were confined to a plane (Saines, 2011). In this experiment, the line segments are freed from the plane and allowed to rotate through both azimuthal and polar angles. This adds an interesting layer of complexity to the problem in the form of two additional parameters that will be discussed in detail below.

II. THEORY

The theory of // is very complex. However, everything up to a certain point is just Newtonian gravitation. For example, Newton postulated and proved that a sphere, at any distance outside of its radius, can be approximated to

have all of its mass concentrated at one point at its center of mass. This is known as the Shell Theorem. If this is true, than a person that wants to know the gravitational attraction between a planet and another body need only to employ the following equation:

$$F = \frac{Gm_1m_2}{r^2}, \quad (1)$$

where G is the gravitational constant, m_1 is one interacting object, m_2 is another interacting object, and r is the distance between their centers of mass. The equation works for planets because they are, to a good approximation, generally spherical. However, in the // body problem, slashes (line segments) can't be approximated as points. They have many different contributing parameters. Their moments of inertia and angular velocities also contribute to their potential energy expression. The expression for the potential energy for the two slashes as they interact is much more complex than it is for spheres or point masses because the Shell Theorem cannot be used. The following expression is that of the potential energy of the slashes with respect to one another:

$$V = -G \frac{m_A m_B}{\ell_A \ell_B} \int_{-\ell_B/2}^{\ell_B/2} \int_{-\ell_A/2}^{\ell_A/2} \frac{1}{\mathfrak{R}} d\delta_A d\delta_B, \quad (2)$$

where G is the gravitational constant, m_A and m_B are the masses of the slashes, ℓ_A and ℓ_B are the lengths of the slashes, δ_A and δ_B are the lengths along the slashes toward the mass elements and \mathfrak{R} is a vector that locates each mass element with respect to the other. The reason there is a double integral is that the entirety of both slashes need to be integrated over, hence the limits of integrations. Spherical polar coordinates are used to do this, so the above expression undergoes a few changes once the transformation to spherical polar coordinates takes place. These changes are discussed in the Procedure section.

Once the potential energy, V , is determined, the kinetic energy, T , must be determined so that the Lagrangian equation ($L = T - V$) can be used (Feynman, 1964). The specific construction of the kinetic energy

will be detailed in the Procedure section as well. However Euler's angles are used and their use is detailed here (Thornton, 2003). Euler's angles are used to describe rotations about three axes, $\dot{\theta}$, $\dot{\phi}$, and $\dot{\psi}$ and rotation through their corresponding angles, θ , ϕ , and ψ . The angle θ governs polar rotations, ϕ governs azimuthal rotations, and ψ governs rotations through the axis parallel to the length of the slash. Since we are dealing with a line segment, the angular velocity about the axis that is parallel to the line segment has no effect on the kinetic energy. This is because a line segment has no thickness. So, the expressions for the angular velocities in the x , y , and z directions become:

$$\begin{aligned}\omega_x &= \dot{\theta}, \\ \omega_y &= \dot{\phi} \sin \theta, \\ \omega_z &= \dot{\phi} \cos \theta.\end{aligned}$$

These expressions are then used in the equation,

$$T_{rot} = \sum \frac{1}{2} I_i \omega_i^2, \quad (3)$$

where I is the moment of inertia ω is the angular velocity, and $i = x, y, z$. From this equation, a large part of the kinetic energy T can be found. The other part comes from what one might expect,

$$T_{lin} = \frac{1}{2} \mu (x'(t)^2 + y'(t)^2), \quad (4)$$

where $\mu = m_A m_B / (m_A + m_B)$ and $x'(t)$ and $y'(t)$ are the velocities in the x and y directions. So then, to find the total kinetic energy, the two parts are summed like so:

$$T_{total} = T_{lin} + T_{rot}. \quad (5)$$

With this background knowledge in place, it is possible to start experimentation with the slashes.

III. PROCEDURE

To begin, it is necessary to define the parameters that will be manipulated throughout the course of the procedure. The lengths of the slashes (or line segments) are denoted by ℓ_A and ℓ_B and the masses are denoted as m_A and m_B . The azimuthal angles for both slashes are denoted as ϕ_A and ϕ_B , respectively, and the polar angles are denoted as θ_A and θ_B , respectively and the physics convention for spherical polar coordinates is used (McQuarrie, 2003). Each slash is divided into mass elements dm_A and dm_B which are located a distance and direction δ_A and δ_B from the center of each slash. There is a vector, $\vec{\mathfrak{R}}$ that locates the mass elements dm_A and dm_B with respect to one another that is defined as $\vec{\mathfrak{R}} = \vec{\delta}_A - \vec{\delta}_B - \vec{r}$, where $\vec{r} = \vec{r}_B - \vec{r}_A$ where \vec{r}_A and \vec{r}_B locate the center of mass of the slash from some arbitrary origin. From

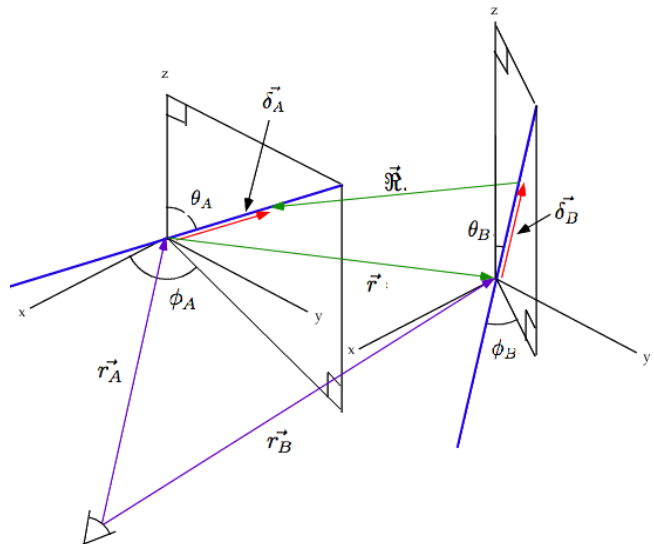


FIG. 1 A diagram of the slashes and relevant parameters.

these basic assignments, we can derive all of the necessary equations for the // problem. A diagram of the system with all of the relevant parameters labeled appears in FIG. 1.

The derivations appear simple but are actually rather complex. The definition for $\vec{\delta}_A$ is as follows:

$$\vec{\delta}_A = \delta_A (\sin \theta_A \cos \phi_A \hat{i} + \sin \theta_A \sin \phi_A \hat{j} + \cos \phi_A \hat{k}). \quad (6)$$

The definition for $\vec{\delta}_B$ is very similar and is as follows:

$$\vec{\delta}_B = \delta_B (\sin \theta_B \cos \phi_B \hat{i} + \sin \theta_B \sin \phi_B \hat{j} + \cos \phi_B \hat{k}). \quad (7)$$

Finally, the definition for $\vec{r} = x \hat{i} + y \hat{j} + 0 \hat{k}$. This definition for \vec{r} actually confines the slashes' centers of mass to the $x - y$ plane. From these definitions the remainder can be input into Mathematica 8 in a very intuitive way i.e. as basic functions of $\vec{\delta}_A$, $\vec{\delta}_B$, and \vec{r} .

Now that all the basic parameters have been defined, it is possible to integrate to find the potential energy V . To do this, an integral of the form,

$$V = -G \frac{m_A m_B}{\ell_A \ell_B} \int_{-\ell_B/2}^{\ell_B/2} \int_{-\ell_A/2}^{\ell_A/2} \frac{1}{\mathfrak{R}} d\delta_A d\delta_B, \quad (8)$$

must be taken. One would assume that with adequate computing power this would be no trouble at all. However, this is not the case. The integral must be broken down into four separate pieces in the following way. First the indefinite integral must be taken with respect to δ_A as follows:

$$\int \frac{1}{\mathfrak{R}} d\delta_A = \text{ResultA} \quad (9)$$

Following this integration, which is fairly quick, the result must be evaluated from $-\ell_A/2$ to $\ell_A/2$ separately, like so:

$$\text{ResultA}|_{+\ell_A/2} - \text{ResultA}|_{-\ell_A/2} = \text{Upper} - \text{Lower}. \quad (10)$$

Then, the result of the previous integral must be taken and integrated two separate times. For clarity I will refer to the integral with respect to δ_A evaluated at $-\ell_A/2$ as “Lower” and evaluated at the upper bound, $\ell_A/2$, as “Upper”. The second integration then looks like

$$\int (Upper - Lower) d\delta_B = \int Upper d\delta_B - \int Lower d\delta_B \quad (11)$$

Then each of these are evaluated at $-\ell_B/2$ and $\ell_B/2$ for a total of four portions known as “Lower-Lower”, “Lower-Upper”, “Upper-Lower”, and “Upper-Upper” (abbreviated as LL, LU, UL, and UU). The final expression for V is

$$V = (UU - UL) - (LU - LL). \quad (12)$$

After completing this integration, it is possible to graph the potential both when ϕ_A and ϕ_B are varied and when θ_A and θ_B are varied. This can be done by setting the other two angles to an arbitrary angle and then using both the Plot3D function and the ContourPlot function in Mathematica 8 for different perspectives on the data.

After this step has been completed, then the potential energy V , and the kinetic energy, T , can be combined using the Lagrangian according to

$$L = T - V. \quad (13)$$

The kinetic energy is here defined as

$$\begin{aligned} T_{total} = & \frac{1}{2} \mu (x'(t)^2 + y'(t)^2) \\ & + \frac{1}{2} \iota_A \theta'_A(t)^2 \\ & + \frac{1}{2} \iota_A (\sin \theta_A(t) \phi'_A(t))^2 \\ & + \frac{1}{2} \iota_A (\cos \theta_A(t) \phi'_A(t))^2 \\ & + \frac{1}{2} \iota_B \theta'_B(t)^2 \\ & + \frac{1}{2} \iota_B (\sin \theta_B(t) \phi'_B(t))^2 \\ & + \frac{1}{2} \iota_B (\cos \theta_B(t) \phi'_B(t))^2, \end{aligned}$$

where ι_A and ι_B are the moments of inertia of the slashes and μ is the reduced mass defined as $m_A m_B / (m_A + m_B)$. The moments of inertia are defined as $\iota_A = (1/12) m_A \ell_A^2$ and $\iota_B = (1/12) m_B \ell_B^2$. The kinetic energy was defined this way because of the definitions of Euler angles and their angular velocities.

Next it is necessary to derive the

force equations for each parameter (i.e. $x(t)$, $y(t)$, $\phi_A(t)$, $\phi_B(t)$, $\theta_A(t)$, $\theta_B(t)$). This is done by taking a series of partial derivatives of the form,

$$\frac{\partial}{\partial t} \frac{\partial L}{\partial x'(t)} = \frac{\partial L}{\partial x(t)}, \quad (14)$$

where each parameter (i.e. x , y , ϕ_A , ϕ_B , θ_A , and θ_B) is put through the above equation individually. After these equations have been created, a numerical differential equation solver using a Symplectic Partitioned Runge-Kutta method is employed to solve these equations for the position variables.

After the equations of motion have been solved for, it will be possible to plot orbits, angular momentum, and even three dimensional spacetime graphs. However, this was not done in this project.

IV. DATA & RESULTS

The first part of data collection was to graph the potential in both a three-dimensional perspective and from a contour perspective. The first potential that was graphed was a special case, where the slashes are confined to a plane (i.e. $\theta_A = \theta_B = \pi/2$). This figure (FIG. 2) was initially plagued with many discontinuities. However, after

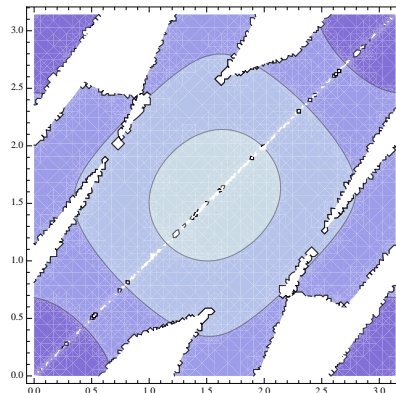


FIG. 2 The unsimplified potential energy in contour form. The different colors denote different heights, lighter being “higher” and darker being “lower”.

considerable simplification, it was possible to pinpoint the sources of the discontinuities and eradicate them. This was done by taking logarithmic combinations such as,

$$\log A - \log B, \quad (15)$$

and substituting,

$$\log \frac{A}{B}. \quad (16)$$

This eliminates any round-off error that would be perpetuated by the subtraction, that is, that the complex

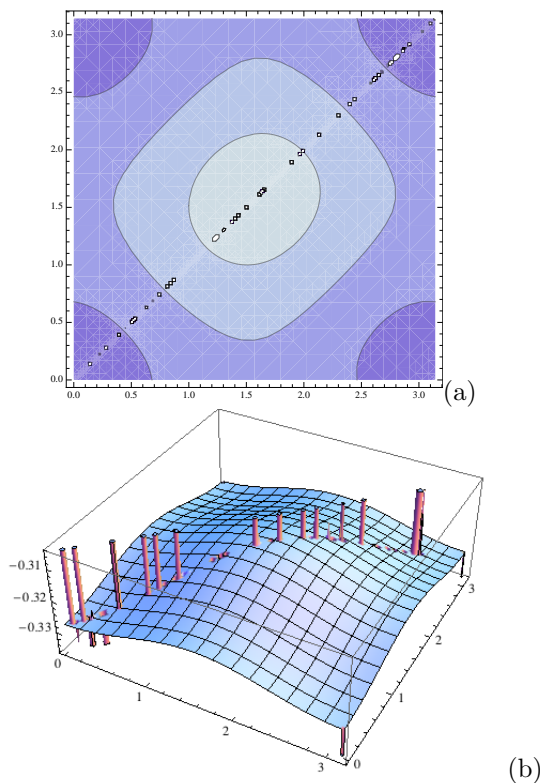


FIG. 3 (a) The simplified potential energy in contour form. The different colors denote different heights, lighter being “higher” and darker being “lower”. The effect of the logarithmic simplification is immediately apparent. (b) A 3D rendering of the same plot.

parts of the logarithms effectively cancel out (Spiegel, 2003). Once these modifications were made to the potential energy expression, the contour plot of V (FIG. 3) is much more continuous, plagued only by a single “scar” across the diagonal. These plots of potential energy were created from the variation of ϕ_A and ϕ_B while holding $\theta_A = \theta_B = \pi/2$. The results pictured in FIG. 3 are consistent with the previous work done by (Saines, 2011). However, the potential can be plotted in a novel way, by varying θ_A and θ_B while holding ϕ_A and ϕ_B at some arbitrary angle as in FIG. 4. From studying the potentials it is possible to conjecture their preferred alignments. For example, here it can be seen that the slashes prefer to be facing each other lengthwise. In the next example, FIG. 5, that the slashes have a larger array of angles that they prefer to be aligned in. In FIG. 6, note that the slashes are near perpendicular to each other and that there appear to be two stable spots in the potential, when $\theta_A = 0$ & $\theta_B = \pi/2$ and when $\theta_A = \pi$ & $\theta_B = \pi/2$. In FIG. 7, set values of the angles have been reversed, so the graph appears to have been rotated $\pi/2$ radians. For three dimensional representations of these plots, see Appendix A.

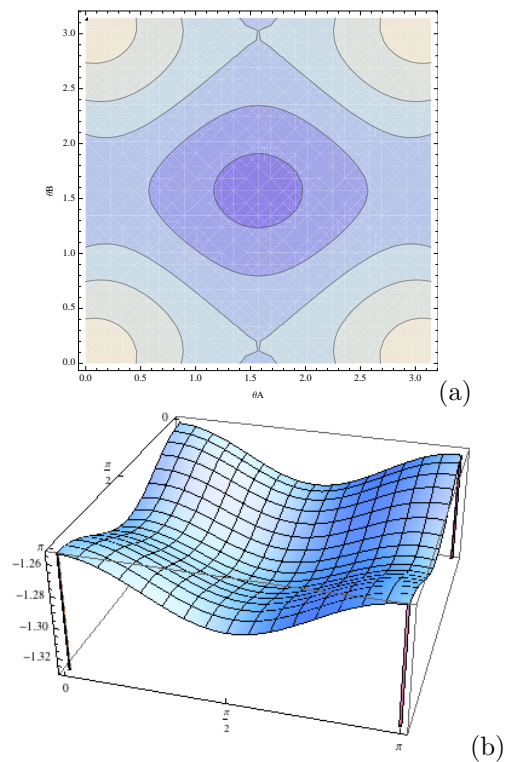


FIG. 4 (a) The potential for θ_A and θ_B , varying from 0 to π , with $\phi_A = \pi/7$ and $\phi_B = \pi/12$. The different colors denote different heights, lighter being “higher” and darker being “lower”. (b) A 3D rendering of the same plot.

V. CONCLUSION

This problem is robust in its complexity. It was found to be possible to integrate the expression for the potential energy as well as the equations of motion. However, it is very difficult to manifest this data into a coherent visualization. The fact that it is possible to derive these equations leaves hope for future investigators who can surely create stunning visualizations of the motion of these line segments. Examples of what could be done include, but are not limited to, animations, spacetime plots and plots for the potential when x and y are allowed to vary. In short, there is plenty more to be done in the regime of the //body problem.

References

- J.M.A. Danby, *Fundamentals of Celestial Mechanics: Second Edition*, (William-Bell, Virginia, 1988).
- John F. Lindner, Jacob Lynn, Frank W. King, & Amanda Logue, *Phys. Rev. E* **81**, 036208, (2010).
- Alex Saines, *//: Order & Chaos in the Rotation & Revolution of Two Line Segments*, (Physics Department, College of Wooster, 2011).
- Richard P. Feynman, Robert B. Leighton, & Matthew Sands, *The Feynman Lectures on Physics Vol. II*, (Pearson, Illi-

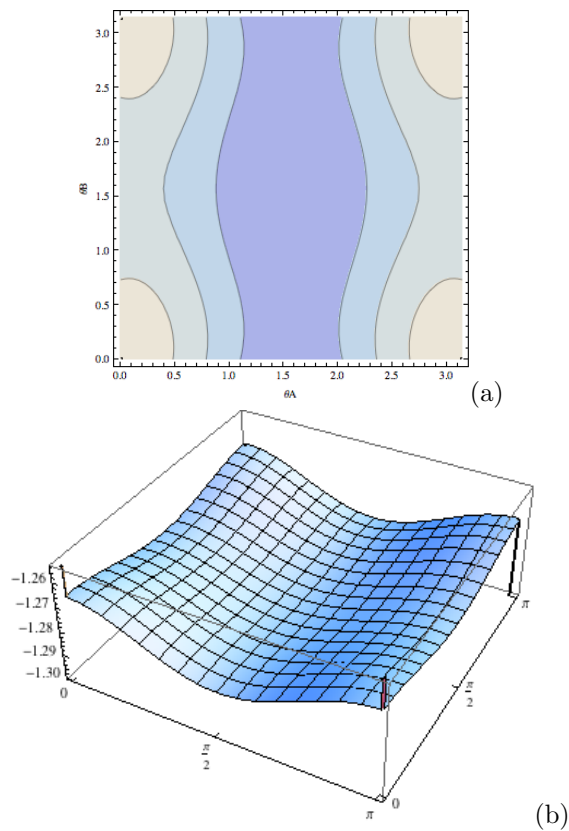


FIG. 5 (a) The potential for θ_A and θ_B , varying from 0 to π , with $\phi_A = \pi/5$ and $\phi_B = \pi/4$. The different colors denote different heights, lighter being “higher” and darker being “lower”. (b) A 3D rendering of the same plot.

nois, 1964).

Stephen T. Thornton & Jerry B. Marion, *Classical Dynamics of Particles and Systems*, (Brooks Cole, 2003).

Donald A. McQuarrie, *Mathematical Methods for Scientists and Engineers*, (University Science Books, California, 2003).

Murray R. Spiegel, Seymour Lipschutz, & John Liu, *Mathematical Handbook of Formulas and Tables Third Edition*, (McGraw-Hill, New York, 2009).

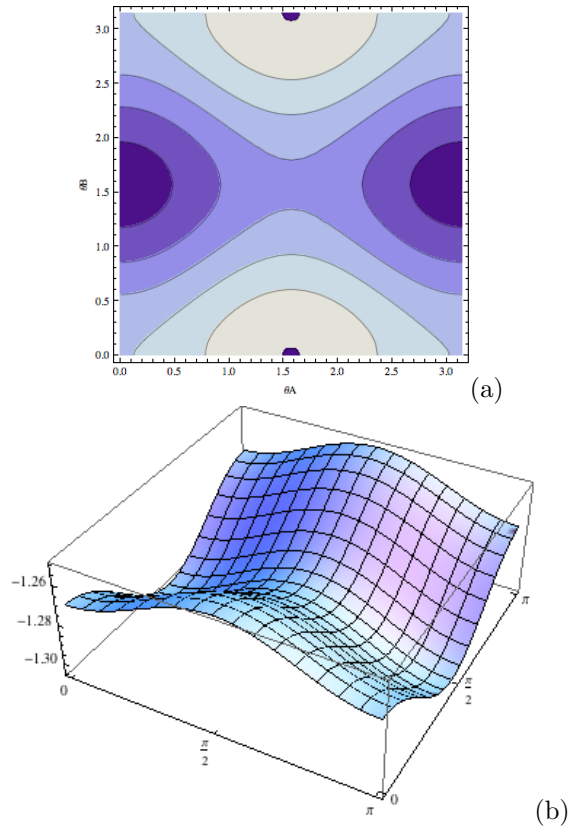


FIG. 6 (a) The potential for θ_A and θ_B , varying from 0 to π , with $\phi_A = \pi/2$ and $\phi_B = \pi/12$. The different colors denote different heights, lighter being “higher” and darker being “lower”. (b) A 3D rendering of the same plot.

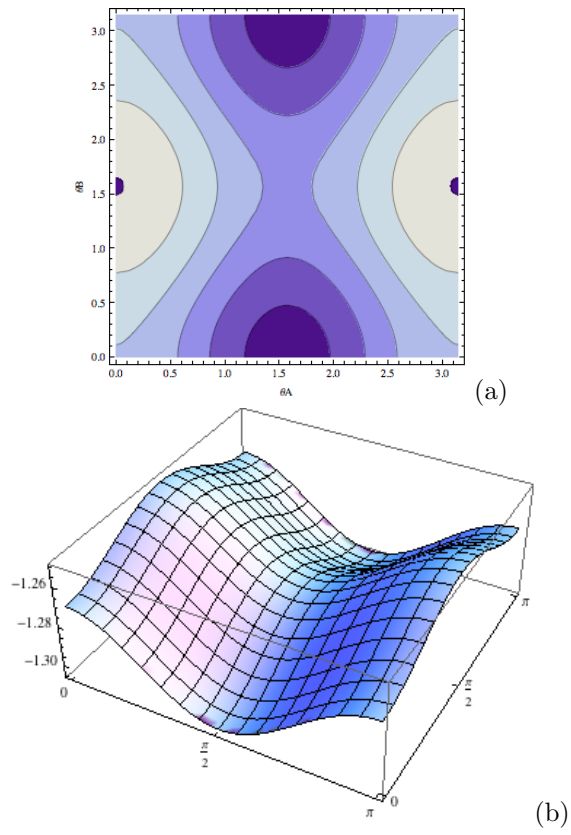


FIG. 7 (a) The potential for θ_A and θ_B , varying from 0 to π , with $\phi_A = \pi/12$ and $\phi_B = \pi/2$. The different colors denote different heights, lighter being “higher” and darker being “lower”. (b) A 3D rendering of the same plot.